



Since January 2020 Elsevier has created a COVID-19 resource centre with free information in English and Mandarin on the novel coronavirus COVID-19. The COVID-19 resource centre is hosted on Elsevier Connect, the company's public news and information website.

Elsevier hereby grants permission to make all its COVID-19-related research that is available on the COVID-19 resource centre - including this research content - immediately available in PubMed Central and other publicly funded repositories, such as the WHO COVID database with rights for unrestricted research re-use and analyses in any form or by any means with acknowledgement of the original source. These permissions are granted for free by Elsevier for as long as the COVID-19 resource centre remains active.



Inhibition of drug-metabolizing enzymes by Qingfei Paidu decoction: Implication of herb-drug interactions in COVID-19 pharmacotherapy

Feng Zhang^{a,1}, Jian Huang^{a,b,1}, Wei Liu^c, Chao-Ran Wang^d, Yan-Fang Liu^d, Dong-Zhu Tu^a, Xin-Miao Liang^d, Ling Yang^a, Wei-Dong Zhang^a, Hong-Zhuan Chen^a, Guang-Bo Ge^{a,*}

^a Institute of Interdisciplinary Integrative Medicine Research, Shanghai University of Traditional Chinese Medicine, Shanghai, China

^b Pharmacology and Toxicology Division, Shanghai Institute of Food and Drug Control, Shanghai, China

^c Institute of Liver Diseases, Shuguang Hospital, Shanghai University of Traditional Chinese Medicine, Shanghai, China

^d Dalian Institute of Chemical Physics, Chinese Academy of Sciences, Dalian, China

ARTICLE INFO

Handling Editor: Dr. Jose Luis Domingo

Keywords:

Qingfei Paidu decoction (QPD)
Cytochrome P450 enzymes (CYPs/P450s)
Herb-drug interactions (HDIs)
CYP3A substrate-drugs

ABSTRACT

Corona Virus Disease 2019 (COVID-19) has spread all over the world and brings significantly negative effects on human health. To fight against COVID-19 in a more efficient way, drug-drug or drug-herb combinations are frequently used in clinical settings. The concomitant use of multiple medications may trigger clinically relevant drug/herb-drug interactions. This study aims to assay the inhibitory potentials of Qingfei Paidu decoction (QPD, a Chinese medicine compound formula recommended for combating COVID-19 in China) against human drug-metabolizing enzymes and to assess the pharmacokinetic interactions *in vivo*. The results demonstrated that QPD dose-dependently inhibited CYPs1A, 2A6, 2C8, 2C9, 2C19, 2D6 and 2E1 but inhibited CYP3A in a time- and NADPH-dependent manner. *In vivo* test showed that QPD prolonged the half-life of lopinavir (a CYP3A substrate-drug) by 1.40-fold and increased the AUC of lopinavir by 2.04-fold, when QPD (6 g/kg) was co-administrated with lopinavir (160 mg/kg) to rats. Further investigation revealed that *Fructus Aurantii Immaturus* (Zhishi) in QPD caused significant loss of CYP3A activity in NADPH-generating system. Collectively, our findings revealed that QPD potentially inactivated CYP3A and significantly modulated the pharmacokinetics of CYP3A substrate-drugs, which would be very helpful for the patients and clinicians to avoid potential drug-interaction risks in COVID-19 treatment.

1. Introduction

Corona Virus Disease 2019 (COVID-19), a newly emerged infective disease, has spread all over the world, with a long incubation period, high infectivity, and general susceptibility to most people (Hamidian and Hamidianjahromi, 2020; Dima et al., 2020; Niu et al., 2020). COVID-19 has brought significantly negative effects for human health. Now researchers are trying to find effective medications (including western therapeutics and herbal medicines) to treat COVID-19, while some therapeutics and herbal medicines have been used for the

treatment or adjuvant treatment of COVID-19 in clinical settings (Luo et al., 2020; Chen et al., 2020; Li et al., 2020a). To fight against COVID-19 in a more efficient way, drug-drug or drug-herb combinations are always used in COVID-19 therapy. In China, several Chinese medicine compound formulas (such as Qingfei Paidu decoction, Jingyin granule and Lianhua Qingwen capsule), have been validated playing an active role in combating this epidemic, especially alleviating the moderate and mild symptoms of some patients (Shi et al., 2020). In most cases, these Chinese Medicines (CMs) are often co-administrated with western therapeutics (such as remdesivir & lopinavir) in COVID-19

Abbreviations: AA, arachidonic acid; AUC, area under the plasma concentration; CES, carboxylesterases; CM, Chinese medicine; CMC-Na, sodium carboxymethyl cellulose; COVID-19, Corona Virus Disease 2019; CYPs/P450s, cytochrome P450 enzymes; DDIs, drug-drug interactions; DMEs, drug-metabolizing enzymes; ESI, electrospray ionization; G-6-P, D-Glucose-6-phosphate; G-6-PDH, glucose-6-phosphate dehydrogenase; HDIs, herb-drug interactions; HLMS, human liver microsomes; IC₅₀, half maximal inhibition concentration; PBS, potassium phosphate buffer; QPD, Qingfei Paidu decoction; RLMS, rat liver microsomes; TCM, Traditional Chinese Medicine; TDI, time-dependent inhibition; t_{1/2}, half-life.

* Corresponding author.

E-mail address: geguangbo@dicp.ac.cn (G.-B. Ge).

¹ These authors contributed equally.

<https://doi.org/10.1016/j.fct.2021.111998>

Received 18 October 2020; Received in revised form 31 December 2020; Accepted 12 January 2021

Available online 19 January 2021

0278-6915/© 2021 Elsevier Ltd. All rights reserved.

treatment. The concomitant use of CMs or herbal medicines with western therapeutics may trigger clinically relevant herb-drug interactions (HDIs) or adverse reactions, thus it is urgent and essential to assess the potential risks of HDIs in COVID-19 treatment.

Among all recommend Chinese medicines for combating COVID-19 in China, Qingfei Paidu decoction (QPD) has drawn much attention owing to its exact effects in COVID-19 treatment. As the first Chinese medicine compound formula recommended by National Health Commission of the People's Republic of China for COVID-19 therapy, QPD has been used to treat thousands of COVID-19 patients with the total effective rate of 97% (Zhang et al., 2020a; Ni et al., 2020; Meng et al., 2020). Following administration of QPD, the major symptoms and imaging manifestations of more than 60% patients were significantly improved, while the symptoms of 30% patients were stable and did not aggravate (Yang et al., 2020). Notably, QPD is a composite of four classic Chinese medicine prescriptions (including Maxing Shigan decoction, Shengan Mahuang decoction, Xiaochaihu decoction, and Wuling powder) that are used for the treatment of epidemic diseases and the related inflammatory symptoms for thousands of years (Li, 2020; Du and Zhang, 2020). As a super combination of 20 herbs and a mineral drug (Gypsum Fibrosum), QPD is composed by hundreds of ingredients which may interact with a panel of human drug-metabolizing enzymes or drug transporters, and then trigger HDIs or other undesirable effects. Currently, various therapeutic agents (such as antiviral drugs, anti-inflammatory drugs, immunosuppressive agents and other western medicines) have been recommended for treating COVID-19 (Gao et al., 2020; Xin et al., 2020; Wang et al., 2020). These therapeutic agents are more likely to be administrated with QPD in clinical settings. Therefore, it is crucial to investigate the potential interactions between QPD and the commonly used therapeutic drugs for treating COVID-19.

It is well-known that most therapeutic drugs (such as remdesivir, lopinavir, etc) used for treating COVID-19 are substrates of phase I drug-metabolizing enzymes (Warren et al., 2016; Kumar et al., 2004), such as cytochrome P450 enzymes (CYPs or P450s) and carboxylesterase (CES). Subsequently, this study aims to investigate the inhibition/inactivation effects of QPD against human phase I drug-metabolizing enzymes, as well as to assess the potential drug-interaction risks when QPD is co-administrated with CYP substrate-drug(s). Following the testing of a panel of *in vitro* inhibition assays, the results clearly demonstrated that QPD dose-dependently inhibited CYPs1A, 2A6, 2C8, 2C9, 2C19, 2D6 and 2E1 but inhibited CYP3A in a time- and NADPH-dependent manner. *In vivo* pharmacokinetic tests showed that QPD could significantly modulate the pharmacokinetics of lopinavir (a CYP3A substrate-drug), when QPD (6 g/kg) was co-administrated with lopinavir (160 mg/kg) to rats. Further investigation revealed that *Fructus Aurantii Immaturus* (Zhishi) in QPD significantly reduced CYP3A activity in a time- and NADPH-dependent manner, suggesting that this herb is a key culprit responsible for CYP3A reduced activity. All these findings offer new insight into the interactions between QPD and therapeutic agents for treating COVID-19, while the key findings presented here are very helpful for the patients and the clinicians to avoid potential drug-interaction risks in COVID-19 treatment.

2. Materials and methods

2.1. Chemicals and reagents

The water extract of QPD (JZT-QFPDT-0318-PG-0321) and the extract from individual herbs for preparing QPD (the preparation procedure and extraction rate of QPD or 21 individual herbs are shown in Table S1) were provided by Jointown Pharmaceutical Group Co.,Ltd. (Shanghai, China). Lansoprazole was purchased from Hairong (Sichuan, China). Mefenamic acid, 6 β -hydroxytestosterone, testosterone, D-glucose-6-phosphate (G-6-P), glucose-6-phosphate dehydrogenase (G-6-PDH), and β -NADP⁺ were obtained from Sigma-Aldrich (St. Louis, MO, USA). Phenacetin, coumarin, paclitaxel, omeprazole,

dextromethorphan, chlorzoxazone, lopinavir and ketoconazole were purchased from Meilun Bio. Tech (Dalian, China). Diclofenac was obtained from Ark Pharm (Wuhan, China). D-luciferin methyl ester (DME) and its hydrolytic metabolite D-luciferin were purchased from AAT Bioquest (USA). N-(2-butyl-1,3-dioxo-2,3-dihydro-1H-phenalen-6-yl)-2-chloroacetamide (NCEN) and its hydrolytic metabolite 4-amino-1,8-naphthalimide (NAH) were synthesized by us according to the previously reported scheme (Jin et al., 2015; Wang et al., 2016). MgCl₂ and sodium carboxymethyl cellulose (CMC-Na) were obtained on Sinopharm Chemical Reagent (Shanghai, China). Luciferin detection reagent (LDR) was ordered from Promega Biotech (Madison, USA). The pooled human liver microsomes (HLMs, Lot No. H0610) from 50 individual donors were supplied by Xenotech (USA). The pooled rat liver microsomes (RLMs, Lot No. JPYX) were from Research Institute for Liver Diseases (RILD, Shanghai, China). LC grade of methanol, acetonitrile and formic acid were ordered from Fisher Scientific Co. (Fair Lawn, NJ, USA), while ultra-purified water was prepared by a Millipore purification system. Each tested compound was dissolved in acetonitrile and each extract was dissolved in ultra-purified water, then stored at -20 °C until use.

2.2. P450 enzyme inhibition assays

2.2.1. Inhibition of P450s by QPD and its individual herbs

P450 inhibition experiments were carried out in 200 μ L reaction mixtures, which included potassium phosphate buffer (PBS, 100 mM, pH 7.4), each P450 substrate, NADPH-generating system (10 mM G-6-P, 1.0 unit/mL G-6-PDH, 1.0 mM β -NADP⁺ and 4.0 mM MgCl₂, HLMs or RLMs, along with inhibitor (Li et al., 2020b; Santori et al., 2020; Salerno et al., 2020; Fang et al., 2020; Zhang et al., 2020b). Each P450 substrate and the details of P450 reactions are shown in Table S2. QPD or its individual herbs (50 μ g/mL-5000 μ g/mL, final concentrations) were added into reaction mixtures to evaluate the inhibitory potentials against P450s. The final concentration of the organic solvent was less than 1% (v/v). The PBS, inhibitors, HLMs or RLMs, and NADPH-generating system were vortexed and then pre-incubated at 37 °C for 3 min or 33 min. The reactions were initiated by adding individual substrates. Reactions proceeded for 10-30 min at 37 °C, and subsequently 200 μ L ice-cold acetonitrile containing internal standard was added to quench the reaction. The mixtures were centrifuged at 20,000 \times g, 4 °C for 20 min, then the supernatant (100 μ L) was mixed with ultrapure water (100 μ L) in a 1:1 ratio for LC-MS/MS analysis as described in Table S2 (please refer to the details in supplementary material).

2.2.2. Inactivation kinetic analyses for time-dependent inhibition

CYP3A inactivation kinetic experiments were carried out as previous reports (Rowland et al., 2011; Kent et al., 2002; Ji et al., 2015). The incubation mixtures consisted of inactivation groups and activity evaluation groups. The inactivation groups (200 μ L) included PBS (pH 7.4), NADPH-generating system, HLMs, and QPD (500-5000 μ g/mL, final concentrations). And the activity evaluation groups (180 μ L) consisted of PBS (pH 7.4), testosterone, and NADPH-generating system. For inactivation groups, the reactions were initiated by adding NADPH-generating system after pre-incubation for 3 min at 37 °C. The inactivation reaction mixtures (20 μ L) were transferred to activity evaluation groups at six time points (0, 5, 10, 15, 20 and 30 min). After the activity evaluation group incubated at 37 °C for 10 min, 200 μ L of ice-cold acetonitrile containing internal standard was added to quench the reaction. The procedures for sample preparation and analysis were identical as above. The natural logarithm of the residual activity (hydroxylated rate of testosterone) was plotted against the pre-incubation time. All inactivation data were fitted by the following equations equation (1):

$$K_{\text{obs}} = K_{\text{inact}} \times I / (I + K_I) \quad (1)$$

where I is concentration of QPD; K_I is the inactivator (QPD)

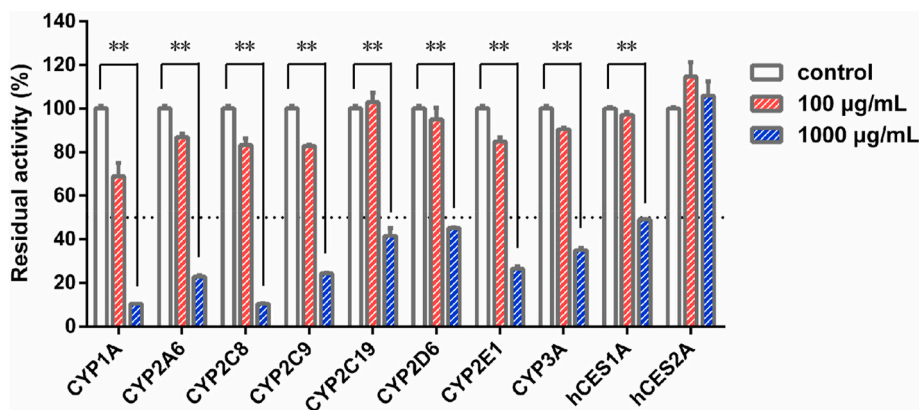


Fig. 1. Inhibition of the major phase I drug-metabolizing enzymes in HLMs by Qingfei Paidu decoction. Data are expressed as mean \pm SD ($n = 3$). ** $P < 0.01$, when compared with the control group.

concentration at half-maximal inactivation; K_{inact} is the maximal inactivation rate constant; K_{obs} is the observed first order inactivation rate constant.

2.3. CES inhibition assays

2.3.1. Inhibition of CES1A-catalyzed DME hydrolysis by QPD

The procedure for hCES1A inhibition assays has been reported previously (Wang et al., 2018; Huo et al., 2020), by using DME as the probe substrate. Briefly, a total of 100 μ L incubation system consisted of PBS (pH 6.5), HLMs, DME and QPD (at different concentrations). The final concentration of the organic solvent was less than 1% (v/v). The PBS, QPD, HLMs were vortexed and pre-incubated at 37 $^{\circ}$ C for 3 or 33 min, then the mixtures were initiated by adding DME and incubated for another 10 min. Then, all reactions were stopped by adding LDR (100 μ L). A fluorescence microplate reader (SpectraMax[®] iD3, Molecular Devices, Austria) was used to measure the hydrolysis rate of DME, via monitoring the formation rates of the hydrolytic metabolite D-luciferin. The details for the hCES1A inhibition assays and the detection conditions for D-luciferin were introduced in Table S3.

2.3.2. Inhibition of CES2A-catalyzed NCEN hydrolysis by QPD

The procedure for hCES2A inhibition assays has also been reported previously (Wang et al., 2018; Song et al., 2019a, 2019b), by using NCEN as the probe substrate. In brief, a total of 200 μ L incubation system consisted of PBS (pH 7.4), HLMs, NCEN and QPD (at different concentrations). The final concentration of the organic solvent was less than 1% (v/v). The PBS, QPD, HLMs were vortexed and pre-incubated at 37 $^{\circ}$ C for 3 or 33 min, then the reactions were initiated by adding NCEN. Meanwhile, the fluorescence microplate reader (SpectraMax[®] iD3, Molecular Devices, Austria) was used to measure the hydrolytic rate of NCEN, via monitoring the formation rates of the hydrolytic metabolite 4-amino-1,8-naphthalimide (NAH). The details for the hCES2A inhibition assays and the detection conditions for NAH were shown in Table S3.

2.4. Pharmacokinetic interactions between QPD and lopinavir in rats

Animal tests were ratified by the Animal Care and Use Committee of Shanghai Institute of Food and Drug Control (approval No. SIFDC18096). Male Sprague-Dawley rats (180–200 g, $n = 6$) were from Shanghai Laboratory Animal Center (Shanghai, China) and were housed at 25 $^{\circ}$ C in a 12 h light-dark cycles at relative humidity \sim 55%. The rats were fasted overnight before dosing, with water freely, and provided food after finishing the study. QPD was suspended in water and lopinavir was suspended in 0.5% CMC-Na. QPD (6 g/kg, $n = 3$) or water (6 g/kg, $n = 3$) was administered intragastrically. After 30 min, lopinavir

(160 mg/kg, $n = 6$) was administered intragastrically (Shi et al., 2013; Ravi and Vats, 2017; Plooy et al., 2011). Blood samples were collected at 0, 0.25, 0.5, 0.75, 1, 2, 3, 4, 6, 8, 12 and 24 h and were centrifuged for 10 min at 8000 rpm at 4 $^{\circ}$ C, and stored at -80 $^{\circ}$ C until analysis. The plasma (20 μ L) was diluted with acetonitrile (containing internal standard) with a ratio of 1:5, and was centrifuged at 20,000 \times g for 30 min at 4 $^{\circ}$ C. 50 μ L supernatant was diluted with 150 μ L Millipore water for LC-MS/MS analysis. The quantification of lopinavir (1–5000 ng/mL) was performed in the linear range of the calibration curve. The pharmacokinetic parameters of lopinavir were fitted by standard non-compartmental analyses using WinNonlin 5.2 (Pharsight Corporation, Mountain View, CA, USA).

2.5. Data analysis

All assays were performed in triplicates, while all data are shown as mean \pm standard deviation (SD). IC_{50} and K_I values were fitted by nonlinear regression in GraphPad Prism 6.0 (GraphPad Software, Inc., La Jolla, USA).

3. Results

3.1. Chemical profiling of QPD by using UHPLC-Q-Exactive Orbitrap HRMS

Firstly, to elucidate the major constituents in QPD, chemical profiling of QPD was conducted by using UHPLC-Q-Exactive Orbitrap HRMS. As shown in Fig. S1 and Table S4, a total of 340 constituents were identified in QPD, which derived from 20 herbs (except Gypsum Fibrosum) contained in the QPD preparation. These QPD constituents were identified (Fig. S1) via comparison with the retention times and MS/MS spectra of the commercially available reference standards, literature and the MS/MS databases of natural products. These constituents could be classified into various classes, including glycosides (111), flavonoids (56), organic acids (37), saponins (34), triterpenoids (24), alkaloids (17), coumarins (10) and others (51). This finding suggests that QPD is a super combination of more than three hundred compounds.

3.2. Inhibitory effects of QPD against DMEs in HLM

Firstly, the inhibitory effects of QPD against ten major human drug-metabolizing enzymes (DMEs) were preliminarily assayed in HLMs, by using three different concentrations (0, 100, and 1000 μ g/mL). As shown in Fig. 1, QPD exhibited negligible inhibitory effect on CES2A-catalyzed NCEN hydrolysis in HLMs. In sharp contrast, QPD displayed relatively strong inhibition on all tested P450s and CES1A. To

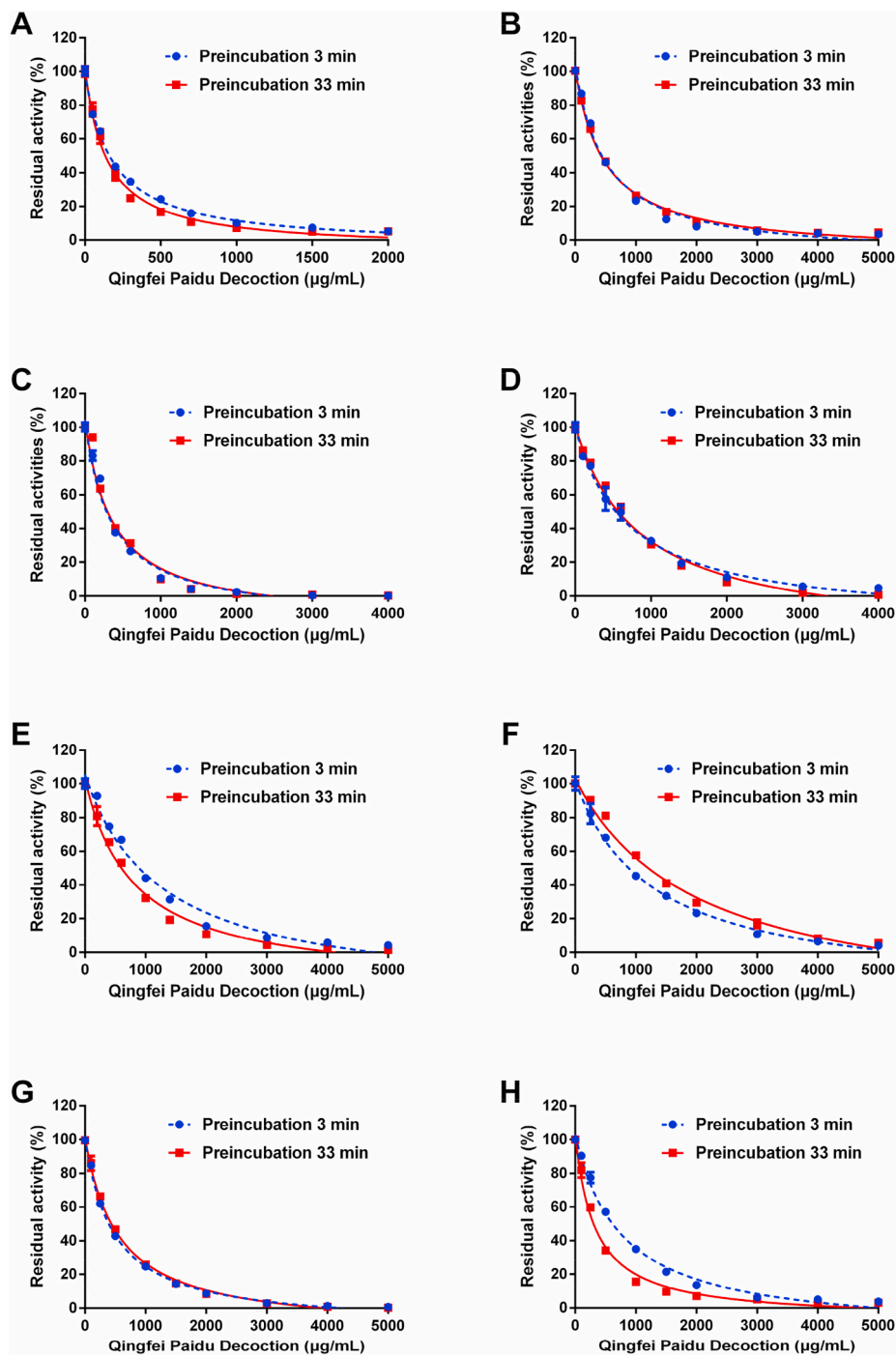


Fig. 2. Dose-inhibition curves of Qingfei Paidu decoction against CYP1A (A), CYP2A6 (B), CYP2C8 (C), CYP2C9 (D), CYP2C19 (E), CYP2D6 (F), CYP2E1 (G) and CYP3A (H) in HLMs, with short (3 min, blue line) or long (33 min, red line) pre-incubation time. Data are expressed as mean \pm SD ($n = 3$). (For interpretation of the references to colour in this figure legend, the reader is referred to the Web version of this article.)

quantitatively measure the inhibitory effects on P450s, dose-inhibition curves of QPD against these DMEs in HLMs were plotted. As shown in Fig. 2, Fig. S2 and Table 1, QPD dose-dependently inhibited CES1A and all tested eight human P450s, with the calculated IC_{50} values as 1336 $\mu\text{g/mL}$, 174.4 $\mu\text{g/mL}$, 498.3 $\mu\text{g/mL}$, 337.7 $\mu\text{g/mL}$, 706.8 $\mu\text{g/mL}$, 1244.0 $\mu\text{g/mL}$, 1253.0 $\mu\text{g/mL}$, 469.3 $\mu\text{g/mL}$, 762.1 $\mu\text{g/mL}$ for CES1A, CYP1A, CYP2A6, CYP2C8, CYP2C9, CYP2C19, CYP2D6, CYP2E1, CYP3A, respectively.

To investigate whether QPD inhibited the activity of DMEs in a time-dependent manner, the effects of different pre-incubation periods on the remaining enzyme activities were assayed in human microsomal

incubations containing QPD. As shown in Fig. 2, Fig. S2 and Table 1, following 33 min pre-incubation at 37 $^{\circ}\text{C}$, QPD dose-dependently inhibited CES1A and eight tested human P450s, with IC_{50} values of 1436 $\mu\text{g/mL}$, 143.3 $\mu\text{g/mL}$, 484.5 $\mu\text{g/mL}$, 355.2 $\mu\text{g/mL}$, 846.7 $\mu\text{g/mL}$, 790.3 $\mu\text{g/mL}$, 1991.0 $\mu\text{g/mL}$, 541.5 $\mu\text{g/mL}$, 324.4 $\mu\text{g/mL}$, respectively. It is evident from these results that co-incubation of QPD with HLMs in the NADPH-generating system for a long period of time could result in significant loss of CYP3A activity (the IC_{50} value was decreased from 762.1 $\mu\text{g/mL}$ to 324.4 $\mu\text{g/mL}$). By contrast, following 33 min pre-incubation, the inhibition potency of QPD against other human CYPs and CES1A became weaker or did not change noticeably (IC_{50} ratio <

Table 1

Inhibitory effects of Qingfei Paidu decoction on major P450s and CES1A (with 3 min or with 33 min pre-incubation) in HLMs.

Probe reaction	Target enzyme	Time-dependent inhibition IC ₅₀ (μg/mL)		Ratio
		Pre-incubation for 3 min	Pre-incubation for 33 min	
Phenacetin O-deethylation	CYP1A	174.4 ± 7.7	143.3 ± 13.0	1.21
Coumarin 7-hydroxylation	CYP2A6	498.3 ± 50.6	484.5 ± 25.3	1.03
Paclitaxel 6α-hydroxylation	CYP2C8	337.7 ± 43.3	355.2 ± 57.9	0.95
Diclofenac 4'-hydroxylation	CYP2C9	706.8 ± 71.1	846.7 ± 92.6	0.83
Omeprazole 5-hydroxylation	CYP2C19	1244.0 ± 201.3	790.3 ± 84.2	1.70
Dextromethorphan O-demethylation	CYP2D6	1253.0 ± 105.7	1991.0 ± 245.5	0.63
Chlorzoxazone 6-hydroxylation	CYP2E1	469.3 ± 24.3	541.5 ± 34.1	0.87
Testosterone 6β-hydroxylation	CYP3A	762.1 ± 65.6	324.4 ± 33.6	2.35
DME-hydrolysis	CES1A	1336.0 ± 173.2	1436.0 ± 192.2	0.93

2.0). These findings suggest that QPD contains naturally occurring CYP3A inactivators, which might inactivate CYP3A activity *in vivo* thus resulting in undesirable effects.

3.3. Inactivation kinetic of QPD against CYP3A in HLMs

Next, the inactivation kinetic analyses of QPD against CYP3A were performed in HLMs, while the inactivation parameters (including K_I and k_{inact} values) were determined in HLMs according to the previously reported method (Fang et al., 2010). In the NADPH-generating system, QPD inactivated CYP3A activity in a dose- and time-dependent manner (Fig. 3). As calculated from the plots present in Fig. 3, the inactivation kinetic constants of QPD against CYP3A, including the K_I and K_{inact} were determined as 1641 μg/mL and 0.032 min⁻¹, respectively. These results clearly demonstrated that QPD inactivates CYP3A activity in a dose-, NADPH- and time-dependent manner, suggesting that QPD may result in undesirable effects *via* inactivation of CYP3A.

3.4. Inactivation of QPD against CYP3A in RLMs

To explore whether QPD shows similar inactivation effects in RLMs as those in HLMs, the inhibitory effects of QPD against CYP3A in RLMs were investigated following pre-incubation at 37 °C during different periods (3 min or 33 min). As shown in Fig. S3, long pre-incubation (33 min) of QPD with RLMs resulted in significant loss of CYP3A activity, the IC₅₀ value was decreased from 706.4 μg/mL to 318.0 μg/mL, resulting in

IC₅₀ ratio of 2.22-fold. These findings clearly demonstrated that QPD inactivates CYP3A in RLMs with very similar inactivation effects as that in HLMs. The pharmacokinetic interactions between QPD and CYP substrate-drugs *in vivo* were studied using rat as a surrogate model for herb-drug interactions in humans.

3.5. Pharmacokinetic interactions between QPD and lopinavir in rats

Encouraged by the above mentioned findings, the *in vivo* effects of QPD on the pharmacokinetic behavior of CYP3A substrate-drug(s) were investigated in rats. Considering that some CYP3A substrate-drugs (such as the antiviral agent lopinavir) are more likely co-administrated with QPD in clinical settings, the pharmacokinetic interactions between QPD and lopinavir were investigated in rats. As shown in Fig. 4 and Table 2. Following co-administration of QPD and lopinavir, the metabolic half-life ($t_{1/2}$) of lopinavir in rats could be prolonged by 40% (from 1.90 h to 2.66 h), while the area under the plasma concentration of lopinavir in rats increased by 2.04-fold (from 6092 ng/mL·h to 12429 ng/mL·h). Moreover, the C_{max} value of lopinavir in rat plasma was slightly increased from 1140 ng/mL to 1190 ng/mL. It is evident from these

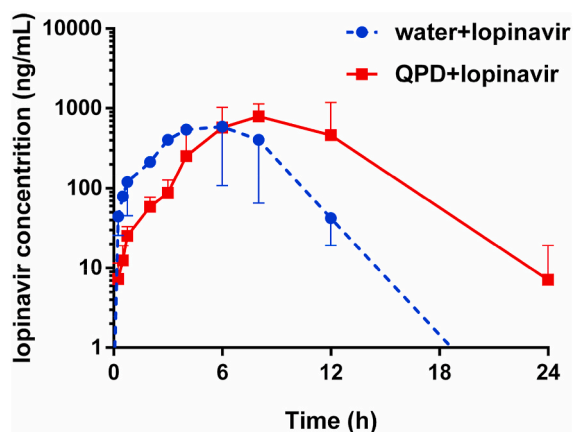


Fig. 4. The mean plasma concentration-time curves of lopinavir (160 mg/kg, i. g.) in control group (water, n = 3) and experimental group (6 g/kg of QPD, i. g., n = 3).

Table 2

Influence of Qingfei Paidu decoction on the pharmacokinetics of lopinavir in rats. Mean ± SD of triplicate rats.

Group	AUC _(0-inf) (ng/mL·h)	C _{max} (ng/mL)	t _{1/2} (h)	T _{max} (h)
Water + lopinavir	6092	1140	1.90	6.00
QPD + lopinavir	12429	1190	2.66	8.00
Ratio	2.04	1.04	1.40	1.33
Increasing (%)	104	4	40	33

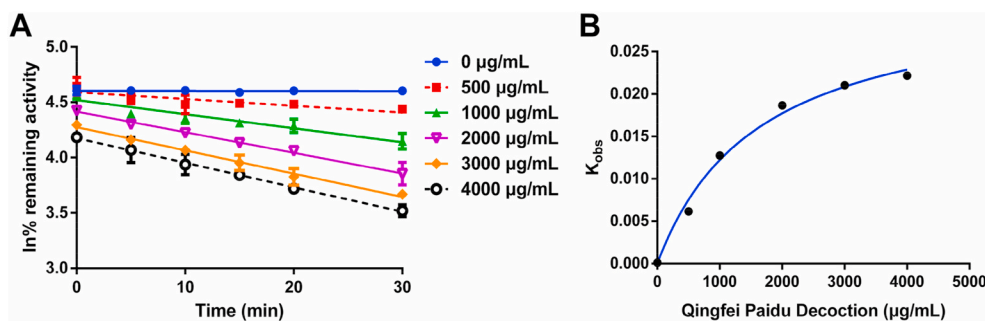


Fig. 3. Time-dependent inhibition of CYP3A by Qingfei Paidu decoction. (A) Time- and dose-dependent inhibition of CYP3A by Qingfei Paidu decoction. (B) The hyperbolic plot of k_{obs} of CYP3A vs. Qingfei Paidu decoction concentrations. Data are expressed as mean ± SD (n = 3).

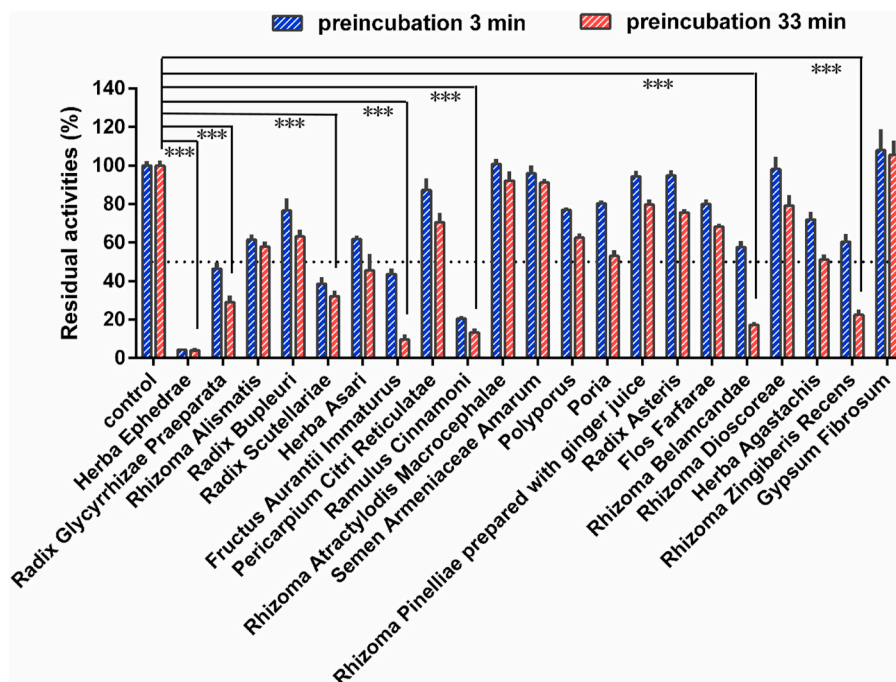


Fig. 5. The inhibitory effects of individual extracts from 21 different herbs used to prepare Qingfei Paidu decoction against CYP3A-catalyzed testosterone 6 β -hydroxylation. Data are expressed as mean \pm SD (n = 3). ***P < 0.001, when compared with the control group.

findings that QPD could strongly modulate the pharmacokinetics of lopinavir in rats, via increasing the plasma exposure to lopinavir prolonging its plasma half-life.

3.6. Inactivation of CYP3A by individual herbs in QPD preparation

To find the key herbs in QPD that caused CYP3A inactivation, time-dependent inhibition of CYP3A by the extract from Gypsum Fibrosum (250 μ g/mL, final concentration) and 20 individual herbs for preparing QPD were conducted. As shown in Fig. 5, seven herbs (including *Herba Ephedrae*, *Radix Glycyrrhizae Praeparata*, *Radix Scutellariae*, *Fructus Aurantii Immaturus*, *Ramulus Cinnamoni*, *Rhizoma Belamcandae*, *Rhizoma Zingiberis Recens*) displayed relatively strong CYP3A inhibition activities, with the residual activities less than 50% in 250 μ g/mL. In this case, the inhibition and inactivation effects of these seven individual herbs for CYP3A were investigated in HLMs. As shown in Fig. 6 and Table 3, *Fructus Aurantii Immaturus*, *Ramulus Cinnamoni*, *Rhizoma Belamcandae*, and *Rhizoma Zingiberis Recens* could inhibit CYP3A-catalyzed testosterone 6 β -hydroxylation in HLMs via a time- and NADPH-dependent manner, with IC₅₀ ratio 7.03-fold, 2.07-fold, 3.11-fold, and 2.82-fold, respectively. Among all tested herbs, *Fructus Aurantii Immaturus* (Zhishi) displayed the most potent CYP3A inactivation potency, with a dramatic 7.03-fold change in IC₅₀ value. This finding suggests that *Fructus Aurantii Immaturus* (Zhishi) is a key herb in QPD resulting in significant loss of CYP3A activity in NADPH-generating system.

4. Discussion

Currently, to fight against COVID-19 in a more efficient way, various drug-drug or drug-herb combinations have been recommended for treating COVID-19 in clinical settings. The concomitant use of drug-herb combinations or CM-drug combinations may trigger clinically relevant drug/herb-drug interactions resulting in adverse drug reactions. As the most popular used Chinese medicine compound formula for combating COVID-19, QPD has been frequently used with other medications (such as antiviral agents) to treat COVID-19 patients. As an extremely complicated CM prescription, QPD contains hundreds of ingredients

which are more likely to interact with a panel of human drug-metabolizing enzymes or drug transporters (Zhao et al., 2020a; Ge, 2019), which in turn may modulate the treatment outcomes (including efficacy and safety) of co-administrated agents and trigger clinically relevant HDIs. Therefore, it is urgent and essential to investigate the inhibition/inactivation potential of QPD against human drug-metabolizing enzymes (DMEs), as well as to assess the potential changes in the pharmacokinetics of co-administrated drug(s) when QPD is co-administrated with western drug(s).

As listed in Table S5, a variety of western drugs including antiviral drugs (such as remdesivir, favipiravir, chloroquine, hydroxychloroquine, nafamostat, camostat, lopinavir and ritonavir) have been recommended for treating COVID-19, these agents are more likely to be co-administrated with QPD in clinical settings. Notably, most of the recommended antiviral drugs are substrates of phase I drug-metabolizing enzymes (such as CYPs and CES). We first investigated the potential interactions between QPD and the key drug-metabolizing enzymes (DMEs) in humans. The results clearly demonstrate that QPD inhibits hCES1A and a series of human P450s. Among all tested DMEs, QPD strongly inhibits CYP1A in a reversible manner, while this Chinese medicine potently inhibits CYP3A in a time- and NADPH-dependent manner. Considering that CYP1A participates in the oxidative metabolism of some important drugs (such as doxofylline) for treating respiratory diseases (Zhao et al., 2020b), QPD may extend the duration time or enhance the plasma exposure of these CYP1A-substrate drugs *in vivo* and modulate their treatment outcomes. Meanwhile, in view of the fact that doxofylline display relatively high safety profiles, inhibition of CYP1A by QPD may enhance the therapeutic efficacy of these agents and hardly trigger serious events of adverse drug reactions. In future, it is necessary to investigate the influence of QPD on the pharmacokinetic profiles of doxofylline or other therapeutic agents (including CYP1A and CYP2C19 substrate drugs) for treating COVID-19, by using suitable *in vivo* surrogate models.

By contrast, inhibition of CYP3A by QPD may trigger clinically relevant HDIs. It is well-known that CYP3A metabolizes ~50% therapeutic agents including many antiviral drugs (such as lopinavir and ritonavir) and some key agents with narrow therapeutic windows (Wu

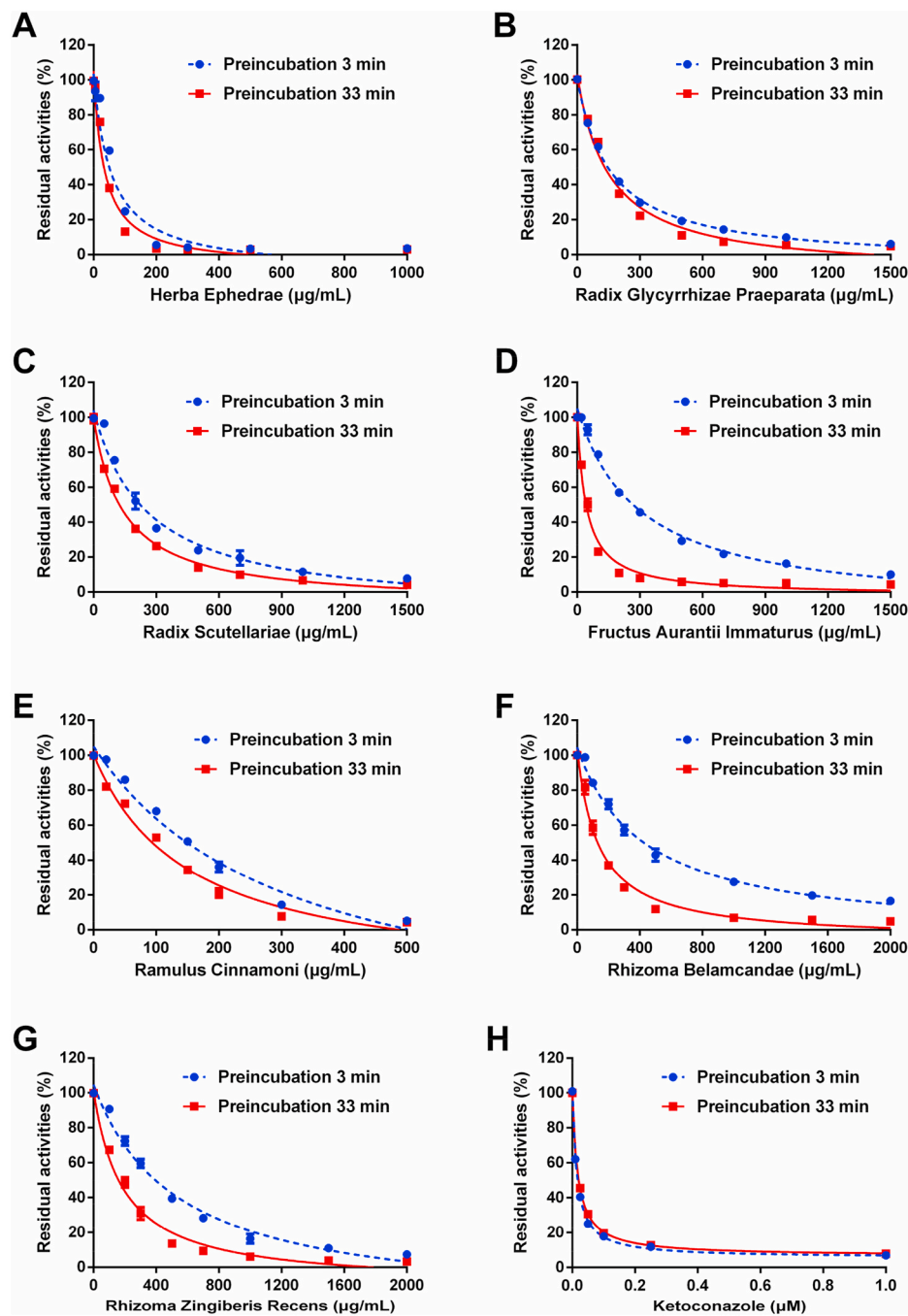


Fig. 6. The inhibitory effects of Herba Ephedrae (A), Radix Glycyrrhizae Praeparata (B), Radix Scutellariae (C), Fructus Aurantii Immaturus (D), Ramulus Cinnamoni (E), Rhizoma Belamcandae (F), and Rhizoma Zingiberis Recens (G) against CYP3A-catalyzed testosterone 6 β -hydroxylation. Figure H depicts the effects of a positive inhibitor ketoconazole against CYP3A-mediated testosterone 6 β -hydroxylation in HLMS. Data are expressed as mean \pm SD (n = 3).

et al., 2021). As a consequence, strong inhibition/inactivation of this key enzyme by QPD may trigger clinically relevant HDIs. Notably, to validate the modulatory effect of QPD on the pharmacokinetic behavior of CYP3A substrate drug(s), an *in vivo* pharmacokinetic test was conducted in the present study. The results showed that QPD (6 g/kg) strongly modulates the pharmacokinetic behavior of lopinavir (160 mg/kg), a CYP3A substrate-drug, via prolongation of the plasma half-life and increase of the plasma exposure (AUC) to this antiviral agent in rats. Meanwhile, it was also clear from Fig. 4 that QPD could affect the adsorption of lopinavir in circulation system. As a result, the T_{max} value of lopinavir was delayed from 6 h to 8 h, when QPD was co-administrated with lopinavir to rats. Such findings could be

explained by the non-specific binding of lopinavir with the crude extract of QPD in the gastrointestinal system, which in turn, delaying the T_{max} value of lopinavir. More recently, a clinical case study reported that QPD could result in hyperkalemia in patients with COVID-19, when QPD is co-administrated with lopinavir/ritonavir (Han et al., 2020). These findings clearly demonstrated that QPD could trigger *in vivo* HDI via inhibition of CYP3A, suggesting that much attention should be paid when QPD was co-administrated with CYP3A substrate drugs. Notably, lopinavir has been reported with various adverse drug reactions (such as diarrhea, nausea, vomiting, blurred vision, epistaxis, hypertriglyceridemia, and Hypercholesterolemia) in clinical settings, thus the dose-related lopinavir ADRs that might become more serious when QPD

Table 3

IC₅₀ values of seven individual herbs for preparing Qingfei Paidu decoction with strong CYP3A inhibition activities.

Herbs	Dose (g)	Extraction rate (%)	Time-dependent inhibition ^a IC ₅₀ (μg/mL)		Ratio
			Pre-incubation for 3 min	Pre-incubation for 33 min	
Herba Ephedrae	9	11.6	55.8 ± 12.9	34.1 ± 6.7	1.64
Radix Glycyrrhizae Praeparata	6	18.5	157.7 ± 7.1	150.3 ± 19.3	1.05
Radix Scutellariae	6	31.2	254.4 ± 38.9	141.4 ± 8.7	1.80
Fructus Aurantii Immaturus	6	14.5	295.9 ± 30.2	42.1 ± 4.4	7.03
Ramulus Cinnamoni	9	5.1	310.7 ± 66.1	150.3 ± 24.9	2.07
Rhizoma Belamcandae	9	9.8	424.1 ± 51.1	136.5 ± 16.3	3.11
Rhizoma Zingiberis Recens	9	4.2	532.8 ± 74.6	188.9 ± 23.1	2.82

^a The IC₅₀ values were determined in HLM following short (3 min) or long (33 min) pre-incubation.

was continuously administrated with lopinavir for several days. Furthermore, the drug reactions may become more serious when QPD is co-administered with some CYP3A-substrate drugs with very narrow therapeutic windows, such as digoxin, warfarin and some anti-cancer agents that are predominantly metabolized by CYP3A.

Notably, inhibition of human P450s is always a double-edged sword. For some agents with very narrow therapeutic indices (such as warfarin and digoxin), inhibition of P450s will trigger undesirable drug/herb-drug interactions. But for some agents with improved safety profiles or wide therapeutic windows, inhibition of the key P450s responsible for metabolic clearance of these agents may extend the metabolic half-lives and increase the plasma exposure of these P450 substrate-drugs *in vivo*, which will be beneficial for the patients. Furthermore, some P450s (such as CYP1A and CYP3A) have been validated as the key enzymes participating in the oxidative metabolism of arachidonic acid (AA) and other fatty acids (Arnold et al., 2010; Kroetz and Zeldin, 2002), while the oxidative metabolites of AA have been recognized as the key chemical mediators of inflammation (Tallima and Ridi, 2017; Fishbein et al., 2020). Thus, potent inhibition on CYP1A and CYP3A by QPD may partially block the formation of the oxidative metabolites of AA, thereby alleviating the systemic inflammation in patients with COVID-19. Thus, at least in part, QPD may exert its anti-inflammatory effects by inhibiting human P450s (mainly on CYP1A and CYP3A). In view of the fact that a set of anti-inflammatory drugs (such as dexamethasone) have been recommended for treating COVID-19 and part of them are CYP substrate-drugs (Tomlinson et al., 1997), the potential interactions between QPD and these anti-inflammatory agents should be carefully investigated from the respects of both pharmacodynamics and pharmacokinetics.

Although this study reports that QPD may inhibit CYP3A both *in vitro* and *in vivo*, it is very difficult to find the key ingredients in QPD that are responsible for CYP3A inhibition. As mentioned above, QPD is a super combination of 21 herbs that composed of hundreds of ingredients, thus it is unfeasible to test the CYP3A inhibition activities of each ingredient in QPD. For this reason, we assayed the inhibitory effects of the water extract of individual herbs on human CYP3A. The results demonstrated that seven herbs in QPD, including *Herba Ephedrae*, *Radix Glycyrrhizae Praeparata*, *Radix Scutellariae*, *Fructus Aurantii Immaturus*, *Ramulus Cinnamoni*, *Rhizoma Belamcandae*, *Rhizoma Zingiberis Recens*, strongly inhibited CYP3A in a dose-dependent manner. Further investigation

demonstrated that *Fructus Aurantii Immaturus*, *Ramulus Cinnamoni*, *Rhizoma Belamcandae*, and *Rhizoma Zingiberis Recens* inhibited CYP3A-catalyzed testosterone 6β-hydroxylation in time-dependent manners, implying that these herbs may contain CYP3A inactivators. Particularly, *Fructus Aurantii Immaturus* (Zhishi) displayed potent CYP3A inactivation potency and triggered a dramatic IC₅₀ shift (7.03-fold change) following different pre-incubation times in NADPH-generating system, suggesting that this herb might be the major culprit in QPD resulting in significant loss of CYP3A activity. Thus, in future, the key ingredients in *Fructus Aurantii Immaturus* (Zhishi) and QPD responsible for CYP3A inhibition/inactivation should be identified and carefully characterized, which will be very helpful for preparing a new herbal remedy to reduce the risks of herb-drug interactions.

5. Conclusion

In summary, the study investigated the inhibitory potentials of QPD against human phase I drug-metabolizing enzymes and assessed the modulatory effects of QPD on the pharmacokinetics of lopinavir *via* inhibiting P450s. The results clearly demonstrated that QPD displayed relatively strong inhibition on all tested P450s and CES1A. Time-dependent inhibition assays showed that QPD inhibit CYP3A-catalyzed testosterone 6β-hydroxylation in a time-dependent manner in liver microsomes of both humans and rats. Further investigation showed that QPD inactivated CYP3A in a dose- and NADPH-dependent manner, with the K_I and K_{inact} (the inactivation kinetic constants) of 1641 μg/mL, and 0.032 min⁻¹, respectively. *In vivo* assays demonstrated that QPD prolonged the half-life of lopinavir by 40% and increased the AUC_(0-inf) (ng/mL·h) of lopinavir by 104%, when QPD (6 g/kg) was co-administrated with lopinavir (160 mg/kg) in rats. In addition, time-dependent inhibition assays of the individual extract from single herbs for preparing QPD demonstrated that *Fructus Aurantii Immaturus* (Zhishi), *Ramulus Cinnamoni* (Guizhi), *Rhizoma Belamcandae* (Shegan), *Rhizoma Zingiberis Recens* (Shengjiang) inhibited CYP3A-catalyzed testosterone 6β-hydroxylation in a time-dependent manner. Among all tested herbs, *Fructus Aurantii Immaturus* (Zhishi) displayed the most potent inactivation effect, suggesting this herb is a key culprit responsible for CYP3A inactivation. Collectively, our findings revealed that QPD could significantly modulate the pharmacokinetic behavior of CYP3A substrate-drugs *via* inactivation of CYP3A in a time- and NADPH-dependent manner, which would help the patients and clinicians to avoid potential drug-interaction risks in COVID-19 treatment. Meanwhile, the key findings present here are also helpful for the developer to optimize the constituted herbs and their ratios, to slow down the risks of herb-drug interactions.

CRedit authorship contribution statement

Feng Zhang: performed the experiments, wrote the manuscript. **Jian Huang:** performed the experiments. **Wei Liu:** performed the experiments. **Chao-Ran Wang:** performed the experiments. **Yan-Fang Liu:** analyzed the data. **Dong-Zhu Tu:** analyzed the data. **Xin-Miao Liang:** analyzed the data. **Ling Yang:** revised the manuscript. **Wei-Dong Zhang:** revised the manuscript. **Hong-Zhuan Chen:** revised the manuscript. **Guang-Bo Ge:** conceived and designed the study, wrote the manuscript, analyzed the data.

Declaration of competing interest

The authors declare that they have no known competing financial interests or personal relationships that could have appeared to influence the work reported in this paper.

Acknowledgement

We'd like to thank Jointown Pharmaceutical Group Co.,Ltd. (China)

for providing QPD extract and 21 single herbs. This work was supported by the National Key Research and Development Program of China (2020YFC0845400, 2017YFC1700200, 2017YFC1702000), the NSF of China (81922070, 81973286), Shanghai Science and Technology Innovation Action Plans (20S21901500; 20S21900900) supported by Shanghai Science and Technology Committee, Program of Shanghai Academic/Technology Research Leader (18XD1403600), the Three-year Action Plan of Shanghai TCM Development (ZY-(2018–2020)-CCX-5001), Shuguang Program (18SG40) supported by Shanghai Education Development Foundation and Shanghai Municipal Education Commission.

Appendix A. Supplementary data

Supplementary data to this article can be found online at <https://doi.org/10.1016/j.fct.2021.111998>.

References

- Arnold, C., Markovic, M., Blossley, K., Wallukat, G., Fischer, R., Dechend, R., Konkel, A., Schacky, C., Luft, F.C., Muller, D.N., Rothe, M., Schunck, W.H., 2010. Arachidonic acid-metabolizing cytochrome P450 enzymes are targets of ω -3 fatty acids. *J. Biol. Chem.* 285 (285), 32720–32733.
- Chen, J., Wang, Y.K., Gao, Y., Hu, L.S., Yang, J.W., Wang, J.R., Sun, W.J., Liang, Z.Q., Cao, Y.M., Cao, Y.B., 2020. Protection against COVID-19 injury by qingfei paidu decoction via anti-viral, anti-inflammatory activity and metabolic programming. *Biomed. Pharmacother.* 129, 110281.
- Dima, M., Enatescu, I., Craina, M., Petre, I., Iacob, E.R., Iacob, D., 2020. First neonates with severe acute respiratory syndrome coronavirus 2 infection in Romania: three case reports. *Medicine (Baltim.)* 14 (99), e21284.
- Du, Y., Zhang, X.G., 2020. Overview of the clinical basis for Qingfei Paidu Decoction in the treatment of new coronavirus pneumonia. *Shaanxi J. Tradit. Chin. Med.* 41, 1016–1019.
- Fang, S.Q., Huang, J., Zhang, F., Ni, H.M., Chen, Q.L., Zhu, J.R., Fu, Z.C., Zhu, L., Hao, W. W., Ge, G.B., 2020. Pharmacokinetic interaction between a Chinese herbal formula Huosuo Yangwei oral liquid and apatinib in vitro and in vivo. *J. Pharm. Pharmacol.* 72, 979–989.
- Fang, Z.Z., Zhang, Y.Y., Ge, G.B., Huo, H., Liang, S.C., Yang, L., 2010. Time-dependent inhibition (TDI) of CYP3A4 and CYP2C9 by nescapine potentially explains clinical nescapine-warfarin interaction. *Br. J. Clin. Pharmacol.* 69, 193–199.
- Fishbein, A., Hammock, B.D., Serhan, C.N., Panigrahy, D., 2020. Carcinogenesis: failure of resolution of inflammation? *Pharmacol. Ther.* 3, 107670.
- Gao, K., Song, Y.P., Chen, H., Zhao, L.T., Ma, L., 2020. Therapeutic efficacy of Qingfei Paidu decoction combined with antiviral drugs in the treatment of corona virus disease 2019: a protocol for systematic review and meta analysis. *Medicine (Baltim.)* 29 (99), e20489.
- Ge, G.B., 2019. Deciphering the metabolic fates of herbal constituents and the interactions of herbs with human metabolic system. *Chin. J. Nat. Med.* 17, 801–802.
- Hamidian, Jahromi A., Hamidianjahromi, A., 2020. Why african Americans are a potential target for COVID-19 infection in the United States. *J. Med. Internet Res.* 12 (22), e19934.
- Han, M.Z., Li, S.S., Li, J., Li, X.C., Gao, L.L., Lu, Y., Zhou, Z.Y., 2020. Qingfei Paidu Decoction induced hyperkalemia in patients with new coronavirus pneumonia. *J. Adverse Drug React.* 22, 375–376.
- Huo, P.C., Guan, X.Q., Liu, P., Song, Y.Q., Sun, M.R., He, R.J., Zou, L.W., Xue, L.J., Shi, J. H., Zhang, N., Liu, Z.G., Ge, G.B., 2020. Design, synthesis and biological evaluation of indanone-chalcone hybrids as potent and selective hCES2A inhibitors. *Eur. J. Med. Chem.* 24, 209, 112856.
- Ji, L., Lu, D., Cao, J., Zheng, L., Peng, Y., Zheng, J., 2015. Psoralen, a mechanism-based inactivator of CYP2B6. *Chem. Biol. Interact.* 5 (240), 346–352.
- Jin, Q., Feng, L., Wang, D.D., Dai, Z.R., Wang, P., Zou, L.W., Liu, Z.H., Wang, J.Y., Yu, Y., Ge, G.B., Cui, J.N., Yang, L., 2015. A two-photon ratiometric fluorescent probe for imaging carboxylesterase 2 in living cells and tissues. *ACS Appl. Mater. Interfaces* 30 (7), 28474–28481.
- Kent, U.M., Aviram, M., Rosenblat, M., Hollenberg, P.F., 2002. The licorice root derived isoflavan glabridin inhibits the activities of human cytochrome P450s 3A4, 2B6, and 2C9. *Drug Metab. Dispos.* 30, 709–715.
- Kroetz, D.L., Zeldin, D.C., 2002. Cytochrome P450 pathways of arachidonic acid metabolism. *Curr. Opin. Lipidol.* 13, 273–283.
- Kumar, G.N., Jayanti, V.K., Johnson, M.K., Uchic, J., Thomas, S., Lee, R.D., Grabowski, B. A., Sham, H.L., Kempf, D.J., Denissen, J.F., Marsh, K.C., Sun, E., Roberts, S.A., 2004. Metabolism and disposition of the HIV-1 protease inhibitor lopinavir (ABT-378) given in combination with ritonavir in rats, dogs, and humans. *Pharm. Res. (N. Y.)* 21, 1622–1630.
- Li, C.H., 2020. Analysis of Qingfei Paidu Decoction in the treatment of new coronavirus pneumonia. *Chin. Folk Ther.* 28, 6–8.
- Li, F., MacKenzie, K.R., Jain, P., Santini, C., Young, D.W., Matzuk, M.M., 2020b. Metabolism of JQ1, an inhibitor of bromodomain and extra terminal bromodomain proteins, in human and mouse liver microsomes. *Biol. Reprod.* 4 (103), 427–436.
- Li, H., Lu, W.L., Sun, Y.N., Xiao, Y., Yang, M., Yang, H.J., Gao, Q.H., Yang, Z.Q., Lu, W.L., Ling, R.J., Shou, Z.X., Hu, J.C., Zhao, X.F., Ma, Y.G., Liu, M.Y., Luo, Z.W., Cheng, B. J., Liu, L., Shen, F., Zhang, S.Y., Zeng, J.Q., Xiang, Y., Huang, C.Q., Yang, Q., Ding, X., Qin, L.X., Wang, R.L., 2020a. Real world clinical study of Chinese medicine treatment of 749 patients with coronavirus disease 2019. *Chin. J. Tradit. Chin. Med.* 35, 3194–3198.
- Luo, E., Zhang, D., Luo, H., Liu, B., Zhao, K., Zhao, Y., Bian, Y., Wang, Y., 2020. Treatment efficacy analysis of traditional Chinese medicine for novel coronavirus pneumonia (COVID-19): an empirical study from Wuhan, Hubei Province, China. *Chin. Med.* 15 (15), 34.
- Meng, J.H., He, Y., Chen, Q., Gao, Q., Chen, Y.G., An, Jing, 2020. A retrospective study of Qingfei Paidu Decoction in the treatment of common/severe new coronavirus pneumonia. *Chin. J. Hosp. Pharm.* 1–7.
- Ni, L., Chen, L., Huang, X., Han, C., Xu, J., Zhang, H., Luan, X., Zhao, Y., Xu, J., Yuan, W., Chen, H., 2020. Combating COVID-19 with integrated traditional Chinese and Western medicine in China. *Acta Pharm. Sin.* B 10, 1149–1162.
- Niu, S., Tian, S., Lou, J., Kang, X., Zhang, L., Lian, H., Zhang, J., 2020. Clinical characteristics of older patients infected with COVID-19: a descriptive study. *Arch. Gerontol. Geriatr.* 89, 104058.
- Plooy, M.D., Viljoen, M., Rheeders, M., 2011. Evidence for time-dependent interactions between ritonavir and lopinavir/ritonavir plasma levels following P-glycoprotein inhibition in Sprague-Dawley rats. *Biol. Pharm. Bull.* 34, 66–70.
- Ravi, P.R., Vats, R., 2017. Comparative pharmacokinetic evaluation of lopinavir and lopinavir-loaded solid lipid nanoparticles in hepatic impaired rat model. *J. Pharm. Pharmacol.* 69, 823–833.
- Rowland, Yeo K., Walsky, R.L., Jamei, M., Rostami-Hodjegan, A., Tucker, G.T., 2011. Prediction of time-dependent CYP3A4 drug-drug interactions by physiologically based pharmacokinetic modelling: impact of inactivation parameters and enzyme turnover. *Eur. J. Pharmaceut. Sci.* 14 (43), 160–173.
- Salerno, S.N., Edginton, A., Gerhart, J.G., Laughon, M.M., Ambalavanan, N., Sokol, G.M., Hornik, C.D., Stewart, D., Mills, M., Martz, K., Gonzalez, D., 2020. Physiologically-Based pharmacokinetic modeling characterizes the CYP3A-mediated drug-drug interaction between fluconazole and sildenafil in infants. *Clin. Pharmacol. Ther.* 21.
- Santori, N., Buratti, F.M., Dorne, J.C.M., Testai, E., 2020. Phosmet bioactivation by isoform-specific cytochrome P450s in human hepatic and gut samples and metabolic interaction with chlorpyrifos. *Food Chem. Toxicol.* 143, 111514.
- Shi, J., Cao, B., Zha, W.B., Wu, X.L., Liu, L.S., Xiao, W.J., Gu, R.R., Sun, R.B., Yu, X.Y., Zheng, T., Li, M.J., Wang, X.W., Zhou, J., Mao, Y., Ge, C., Ma, T., Xia, W.J., Ai, J.Y., Wang, G.J., Liu, C.X., 2013. Pharmacokinetic interactions between 20(S)-ginsenoside Rh2 and the HIV protease inhibitor ritonavir in vitro and in vivo. *Acta Pharmacol. Sin.* 34, 1349–1358.
- Shi, N., Liu, B., Liang, N., Ma, Y., Ge, Y., Yi, H., Wo, H., Gu, H., Kuang, Y., Tang, S., Zhao, Y., Tong, L., Liu, S., Zhao, C., Chen, R., Bai, W., Fan, Y., Shi, Z., Li, L., Liu, J., Gu, H., Zhi, Y., Wang, Z., Li, Y., Li, H., Wang, J., Jiao, L., Tian, Y., Xiong, Y., Huo, R., Zhang, X., Bai, J., Chen, H., Chen, L., Feng, Q., Guo, T., Hou, Y., Hu, G., Hu, X., Hu, Y., Huang, J., Huang, Q., Huang, S., Ji, L., Jin, H., Lei, X., Li, C., Wu, G., Li, J., Li, M., Li, Q., Li, X., Liu, H., Liu, J., Liu, Z., Ma, Y., Mao, Y., Mo, L., Na, H., Wang, J., Song, F., Sun, S., Wang, D., Wang, M., Wang, X., Wang, Y., Wang, Y., Wu, W., Wu, L., Xiao, Y., Xie, H., Xu, H., Xu, S., Xue, R., Yang, C., Yang, K., Yang, P., Yuan, S., Zhang, G., Zhang, J., Zhang, L., Zhao, S., Zhao, W., Zheng, K., Zhou, Y., Zhu, J., Zhu, T., Li, G., Wang, W., Zhang, H., Wang, Y., Wang, Y., 2020. Association between early treatment with Qingfei Paidu decoction and favorable clinical outcomes in patients with COVID-19: a retrospective multicenter cohort study. *Pharmacol. Res.* 161, 105290.
- Song, Y.Q., Guan, X.Q., Weng, Z.M., Wang, Y.Q., Chen, J., Jin, Q., Fang, S.Q., Fan, B., Cao, Y.F., Hou, J., Ge, G.B., 2019a. Discovery of a highly specific and efficacious inhibitor of human carboxylesterase 2 by large-scale screening. *Int. J. Biol. Macromol.* 15 (137), 261–269.
- Song, Y.Q., Weng, Z.M., Dou, T.Y., Finel, M., Wang, Y.Q., Ding, L.L., Jin, Q., Wang, D.D., Fang, S.Q., Cao, Y.F., Hou, J., Ge, G.B., 2019b. Inhibition of human carboxylesterases by magnolol: kinetic analyses and mechanism. *Chem. Biol. Interact.* 308, 339–349.
- Tallima, H., Ridi, R., 2017. Arachidonic acid: physiological roles and potential health benefits-A review. *J. Adv. Res.* 24 (11), 33–41.
- Tomlinson, E.S., Lewis, D.F., Maggs, J.L., Kroemer, H.K., Park, B.K., Back, D.J., 1997. In vitro metabolism of dexamethasone (DEX) in human liver and kidney: the involvement of CYP3A4 and CYP17 (17,20 LYASE) and molecular modelling studies. *Biochem. Pharmacol.* 54, 605–611.
- Warren, T.K., Jordan, R., Lo, M.K., Ray, A.S., Mackman, R.L., Soloveva, V., Siegel, D., Perron, M., Bannister, R., Hui, H.C., Larson, N., Strickley, R., Wells, J., Stuthman, K. S., Van Tongeren, S.A., Garza, N.L., Donnelly, G., Shurtleff, A.C., Retterer, C.J., Gharaibeh, D., Zamani, R., Kenny, T., Eaton, B.P., Grimes, E., Welch, L.S., Gomba, L., Wilhelmssen, C.L., Nichols, D.K., Nuss, J.E., Nagle, E.R., Kugelmann, J.R., Palacios, G., Doerfler, E., Neville, S., Carra, E., Clarke, M.O., Zhang, L., Lew, W., Ross, B., Wang, Q., Chun, K., Wolfe, L., Babusis, D., Park, Y., Stray, K.M., Trancheva, I., Feng, J.Y., Barauskas, O., Xu, Y., Wong, P., Braun, M.R., Flint, M., McMullan, L.K., Chen, S.S., Fearn, R., Swaminathan, S., Mayers, D.L., Spiropoulou, C.F., Lee, W.A., Nichol, S.T., Cihlar, T., Bavari, S., 2016. Therapeutic efficacy of the small molecule GS-5734 against Ebola virus in rhesus monkeys. *Nature* 17 (531), 381–385.
- Wang, D.D., Jin, Q., Zou, L.W., Hou, J., Lv, X., Lei, W., Cheng, H.L., Ge, G.B., Yang, L., 2016. A bioluminescent sensor for highly selective and sensitive detection of human carboxylesterase 1 in complex biological samples. *Chem. Commun.* 21 (52), 3183–3186.
- Wang, L., Xu, X., Ruan, J., Lin, S., Jiang, J., Ye, H., 2020. Quadruple therapy for asymptomatic COVID-19 infection patients. *Expert Rev. Anti Infect. Ther.* 18, 617–624.

- Wang, Y.Q., Weng, Z.M., Dou, T.Y., Hou, J., Wang, D.D., Ding, L.L., Zou, L.W., Yu, Y., Chen, J., Tang, H., Ge, G.B., 2018. Nevadensin is a naturally occurring selective inhibitor of human carboxylesterase 1. *Int. J. Biol. Macromol.* 120, 1944–1954.
- Wu, J.J., Guan, X.Q., Dai, Z.R., He, R.J., Ding, X.X., Yang, L., Ge, G.B., 2021. Molecular probes for human cytochrome P450 enzymes: Recent progress and future perspectives. *Coord. Chem. Rev.* 427, 213600.
- Xin, S., Cheng, X., Zhu, B., Liao, X., Yang, F., Song, L., Shi, Y., Guan, X., Su, R., Wang, J., Xing, L., Xu, X., Jin, L., Liu, Y., Zhou, W., Zhang, D., Liang, L., Yu, Y., Yu, R., 2020. Clinical retrospective study on the efficacy of Qingfei Paidu decoction combined with Western medicine for COVID-19 treatment. *Biomed. Pharmacother.* 129, 110500.
- Yang, R., Liu, H., Bai, C., Wang, Y., Zhang, X., Guo, R., Wu, S., Wang, J., Leung, E., Chang, H., Li, P., Liu, T., Wang, Y., 2020. Chemical composition and pharmacological mechanism of qingfei paidu decoction and ma xing shi Gan decoction against coronavirus disease 2019 (COVID-19): in silico and experimental study. *Pharmacol. Res.* 157, 104820.
- Zhang, F., Huang, J., He, R.J., Wang, L., Huo, P.C., Guan, X.Q., Fang, S.Q., Xiang, Y.W., Jia, S.N., Ge, G.B., 2020b. Herb-drug interaction between Styraex and warfarin: molecular basis and mechanism. *Phytomedicine* 77, 153287.
- Zhang, Y., Xie, H., Li, Y., Li, T., Yuan, H., Fu, X., Xie, C., 2020a. Qingfei Paidu decoction for treating COVID-19: a protocol for a meta-analysis and systematic review of randomized controlled trials. *Medicine (Baltim.)* 4 (99), e22040.
- Zhao, J., Tian, S.S., Lu, D., Yang, J., Zeng, H.W., Zhang, F., Tu, D.Z., Ge, G.B., Zheng, Y.J., Shi, T., Xu, X., Zhao, S.Y., Yang, Y.L., Zhang, W.D., 2020a. Systems pharmacological study illustrates the immune regulation, anti-infection, anti-inflammation, and multi-organ protection mechanism of Qing-Fei-Pai-Du decoction in the treatment of COVID-19. *Phytomedicine* 9, 153315.
- Zhao, X.H., Ma, H., Pan, Q.S., Wang, H.Y., Qian, X.K., Song, P.F., Zou, L.W., Mao, M.Q., Xia, S.Y., Ge, G.B., Yang, L., 2020b. Theophylline acetaldehyde as the initial product in doxophylline metabolism in human liver. *Drug Metab. Dispos.* 48, 345–352.